

Lead Acid Battery Analysis using S-Transform

Muhammad Sufyan Safwan Mohamad Basir¹, Abdul Rahim Abdullah¹, Nur Asmiza Selamat¹
Haslinda Musa², Rahifa Ranom¹

¹Center for Robotics and Industrial Automation (CeRIA), Faculty of Electrical Engineering, Universiti Teknikal Malaysia Melaka, Durian Tunggal, Malacca, 76100, Malaysia
E-mail: muhammadsufyan91@gmail.com

²Centre of Technopreneurship Development (C-TeD), Universiti Teknikal Malaysia Melaka, Hang Tuah Jaya, 76100 Durian Tunggal, Melaka, Malaysia

Abstract— This paper proposes a new signal processing technique using time-frequency distribution (TFD), namely S-transform (ST) for battery parameters estimation. Compared to other TFDs such as short time Fourier transform (STFT) and wavelet transform (WT), ST technique offers more promising results in a low frequency application analysis, especially battery. The results of the ST are the parameters of instantaneous means square voltage ($V_{RMS}(t)$), instantaneous direct current voltage ($V_{DC}(t)$) and instantaneous alternating current voltage ($V_{AC}(t)$) extracted from the time-frequency representation (TFR). Simulation through MATLAB has been conducted using equivalent circuit model (ECM), using 12 V lead acid (LA) battery with capacities from 1.0 Ah to 10.0 Ah. For the battery model, charging/discharging signal has been used to estimate the battery parameters from the ST technique to determine battery characteristics. From the signal characteristics of battery capacity versus $V_{AC}(t)$ obtained, new equation is proposed based on the curve fitting tool. The advantage of this technique embraces a better capability in estimating battery parameters at low frequency component, resulting in better frequency and time resolutions compared to previous TFDs.

Keywords— lead acid; equivalent circuit model; S-Transform; time-frequency representation

I. INTRODUCTION

Lead acid (LA) battery is the first type of battery, manufactured in the early 1880s. The founder, Gaston Plante, invented the first LA at the French Academy of Sciences in 1860, where the concept is by polarisation between two identical lead plates immersed in 10% sulphuric acid solution [1]. The processes of charging and discharging of an LA battery occur through the chemical reaction at the positive and negative electrode using sulphuric acid (H_2SO_4). During the charging process, chemical substances of lead dioxide (PbO_2) are at the positive electrode, while lead (Pb) is attached to the negative electrode. However, during the discharging process, sulphate substance (SO_4) is collected at both positive and negative electrodes [2]. In a study done by [3], they discovered the occurrence of corrosion, acid stratification and gassing phenomena, which directly affect battery aging due to the charging/discharging cycles of an LA battery. An example of negative effect from these phenomena is when the battery terminal voltage degrades, and temperature rises due to the increasing value of the internal resistance of battery. For telecom users, LA battery is the most preferred choice as a backup power due to its low

investment cost [4]. Moreover, the characteristics of being light weight and having good discharge performance are crucial for certain applications, especially in the automotive industry [5].

Signal processing techniques are widely adapted in many engineering applications, such as power quality, radar, sonar and telecommunication, in which the analysis of time-varying stationary and nonstationary signals are presented in frequency domain [6]. Lately, signal processing technique, such as Fourier transform, has been implemented to analyse batteries in improving their performance through state of charge (SOC) determination [7], [8]. The implementation of Fourier transform is to overcome the limitation of a conventional battery analysis techniques, that were actually the extension of Kalman filter and Coulomb counting, which originally were disadvantageous in terms of computational burden, time consumption and real-time application [9]. Linear time-frequency distribution (TFD) techniques have been proposed to overcome the limitations and inadequacy of Fourier transform in determining the modification within the magnitude, frequency or phase [10], [11]. There are several linear TFDs, i.e. short time Fourier transform (STFT), wavelet transform (WT) and S-transform (ST) [12].

STFT has been proposed to overcome the limitation of Fourier transform in non-stationary signal analysis [13], [14]. In the late 1940s and early 1970s, STFT was proposed by Dennis Gabor [15], [16] by adapting the Fourier analysis to small segments of signals. From the assumption of stationary signal position by dividing the time of analysis in intervals [17], [18], researchers in [19] implemented this concept in estimating the battery parameters, namely instantaneous RMS voltage ($V_{RMS}(t)$), direct current voltage ($V_{DC}(t)$) and alternating current voltage ($V_{AC}(t)$) in the joint time-frequency domain. Analysis using the STFT has the advantages of the best performance result in resolution, fast computation and frequency selectivity [20], [21]. STFT is a common method used in monitoring time variations of waveform distortions by providing the information of time variations of individual components precisely. STFT depends on the width of the window function to localize time and frequency. The time frequency resolution can be adjusted by setting the size of the windows [22], [23]. However, using a fixed size of window has some disadvantages, because the small size of window will result in low frequency resolution that is inappropriate for battery analysis, which has frequency components near zero. Somehow, using bigger size of the window also leads to poor time resolution required in determining the health status of the battery.

WT is a mathematical function created in the early 19th century [24], [25]. WT technique is classified into two (2) forms: the first is the continuous wavelet transform (CWT), and the second is discrete wavelet transform (DWT). DWT can be viewed as a subset of CWT [26]. Their principals are similar to those of Fourier analysis, but are more capable to handle some of their commonly associated constrains [27]. WT is generally more superior compared to other spectral analysis techniques. The power of wavelets comes from the use of multi resolution frequency. WT measures low frequency component using wider window size, and high frequency components using narrow window. This multi-resolution window ensures consistent analysis signal for both time and frequency resolution [28]. However, this technique has a weakness, in which the mother wavelet may face difficulty to select different types of battery to avoid getting inaccurate results, since each battery has different properties [29] - [31].

ST is usually used to solve problems in case of other linear TFDs such as STFT, Gabor transform and WT, particularly in examining the time-varying nature of the spectrum [32]. ST also shows promising results not only in PQ disturbance, but also in other applications such as biomedical. Based on the results made by researchers in [33], ST is capable to emphasize on heart impulses better than STFT. The strength of ST in time-frequency localized also makes this technique useful in data adaptive filters [34]. Besides, ST has the ability to retain the original signal phase, as well as the capability to detect the lossless inverse transformation, compared to WT [35]. Using mathematical mechanism in extracting the information of time and frequency, ST can also be applied in PQ disturbance application [36]. ST constructions are by hybridizing the elements of STFT and WT [37]. This technique is closely related to continuous WT, where the element of Morlet

mother wavelet from separation of frequency band is used in determining the frequency components [10], [11]. Except for multiresolution strategy, ST formula is similar to STFT in its way of preserving the phase information. The window width varies with the frequency measured [12], thus, higher frequency resolution by low frequency component and good time resolution by high frequency component can be achieved through the window function [38].

The performance of linear TFD techniques which are STFT, WT and ST used in signal processing based on the review than had been made are summarized in Table I.

TABLE I
SIGNAL PROCESSING TECHNIQUES SUMMARY

| Technique | Summary |
|-------------------|---|
| Spectrogram | <ul style="list-style-type: none"> • Can be used to analyse non-stationary signal • Fixed window length comprises of time and frequency resolution • Analysis signal is represented in three dimensional TFR |
| Wavelet Transform | <ul style="list-style-type: none"> • Use frequency-dependent window where long window resulting in low frequency resolution and short window yields high frequency resolution. • Sensitive to noise • High memory and computational complexity |
| S-Transform | <ul style="list-style-type: none"> • Inheriting both spectrogram and wavelet transform elements • Capable to analyse low frequency components. • High computational complexity |

This paper presents analysis on LA battery charging/discharging signals, using signal processing technique, namely ST. In this method, the battery charging/discharging signals were generated from equivalent circuit model (ECM) for 900 seconds of charging and discharging for 5 cycles, based on the standard by the Institute of Electrical and Electronics Engineers (IEEE) standard 1188-2005. For the analysis signal, 12 V LA model with capacity from 1.0 Ah to 10.0 Ah were simulated in MATLAB Simulink. Then, the battery charging/discharging signals were analysed using ST, then presented in three-dimensional graph known as time-frequency representation (TFR). From the TFR, battery parameters, namely instantaneous means square voltage ($V_{RMS}(t)$), instantaneous direct current voltage ($V_{DC}(t)$), and instantaneous alternating current voltage ($V_{AC}(t)$), were estimated. Based on the $V_{AC}(t)$ obtained from AC components, the battery characteristics were predicted to determine its storage capacity.

II. MATERIAL AND METHOD

A. Equivalent Circuit Model

Different types of batteries have different charging/discharging characteristics. This research was carried out specifically using lead acid (LA) battery. ECM approach was used to generate the charging/discharging

signals using MATLAB Simulink. The internal structure of the battery is represented by a single internal resistance, following the concept of Rint ECM. This model is capable to give an accurate prediction of SOC and state of discharge (SOD) of the battery. Equations of charging/discharging signals of LA based on ECM as proposed by [39] will then be defined, respectively as

Charging:

$$V_t = E_0 - K \frac{Q}{Q-it} it - K \frac{Q}{it-0.1Q} i - Ri + \exp(t) \quad (1)$$

Discharging:

Where

$$V_t = E_0 - K \frac{Q}{Q-it} it - K \frac{Q}{Q-it} i - Ri + \exp(t) \quad (2)$$

TABLE II

ECM BATTERY PARAMETERS

| Capacity (Ah) | Constant Voltage (V) | Internal Resistance (Ω) | Polarization Resistance (Ω) | Fully Charged Voltage (V) | Exponential Zone Voltage (V) | Exponential Zone Capacity (Ah) |
|---------------|----------------------|-------------------------|-----------------------------|---------------------------|------------------------------|--------------------------------|
| 1.0 | 12.1573 | 0.1200 | 0.1834 | 13.2200 | 12.1500 | 0.0033 |
| 2.0 | 12.1499 | 0.0600 | 0.0866 | 13.3200 | 12.1500 | 0.0067 |
| 3.0 | 12.1424 | 0.0400 | 0.0543 | 13.4200 | 12.1500 | 0.0100 |
| 4.0 | 12.1350 | 0.0300 | 0.0382 | 13.5200 | 12.1500 | 0.0133 |
| 5.0 | 12.1305 | 0.0240 | 0.0293 | 13.5800 | 12.1500 | 0.0167 |
| 6.0 | 12.1276 | 0.0200 | 0.0238 | 13.6200 | 12.1500 | 0.0200 |
| 7.0 | 12.1231 | 0.0171 | 0.0195 | 13.6800 | 12.1500 | 0.0233 |
| 8.0 | 12.1186 | 0.0150 | 0.0163 | 13.7400 | 12.1500 | 0.0267 |
| 9.0 | 12.1149 | 0.0133 | 0.0139 | 13.7900 | 12.1500 | 0.0300 |
| 10.0 | 12.1112 | 0.0120 | 0.0120 | 13.8400 | 12.1500 | 0.0333 |

B. S-Transform

Although Cohen class bilinear TFD can give accurate estimation for nonlinear signal from the cross term artefacts, ST has an extra advantage, as it has better performance in term of high noise ratio (SNR) signals from the adaptation of the Gaussian window [40]. The ST offers absolutely-referenced frequency and phase information to produce three-dimensional TFR [41], and is expressed as

$$ST_x(\tau, f) = \int_{-\infty}^{\infty} x(t) w(\tau-t, f) e^{-j2\pi ft} dt \quad (4)$$

$$w(\tau) = \frac{1}{\sigma\sqrt{2\pi}} e^{-\frac{\tau^2}{2\sigma^2}} \quad (5)$$

$$\sigma(f) = \frac{1}{|f|} \quad (6)$$

The final expression becomes

$$ST_x(\tau, f) = \int_{-\infty}^{\infty} x(t) \frac{|f|}{\sqrt{2\pi}} e^{-((\tau-t)^2 f^2 / 2)} e^{-j2\pi ft} dt \quad (7)$$

where $x(t)$ is the signal, i is the time, f is the frequency, $w(t)$ is the scalable Gaussian window, and $\sigma(f)$ is a parameter which controls the position of the Gaussian window on the x-axis. From the ST equation, the Gaussian part acts as a frequency sensitive window function. If high frequency occurs at the measured signal $x(t)$, the Gaussian window will be narrow, whereas if low frequency occur at the input signal, the window will become wider. Therefore, ST can cover multi-resolution frequency components from variable-width Gaussian window [13]-[15].

Fig. 1 shows the variation of windows used in ST technique. As can be seen, wider window length (512) gives better frequency resolution and benefit for lower frequency application. Narrow window length (64) provides good time

resolution for high frequency. So, variety of window length provides better accuracy in multi-frequency application.

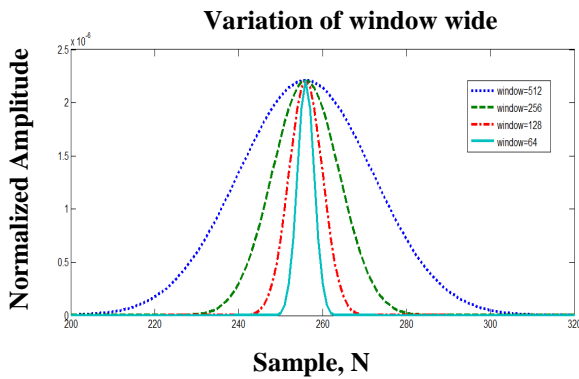


Fig. 1 Variation of window length

Results of ST which is TFR of a time series is from the combination of frequency-dependent resolution that concurrently localized the real and imaginary signals. From the Gaussian modulated cosinusoidal, time-frequency spectrum is represented from intuitive notions of cosinusoidal frequencies [12]. In Fig. 2, the frequency and time resolution relates to window length. Selecting wider window gives advantages in frequency resolution from the horizontal plane and narrow window resulting in good time resolution from the vertical plane based on Fig. 2.

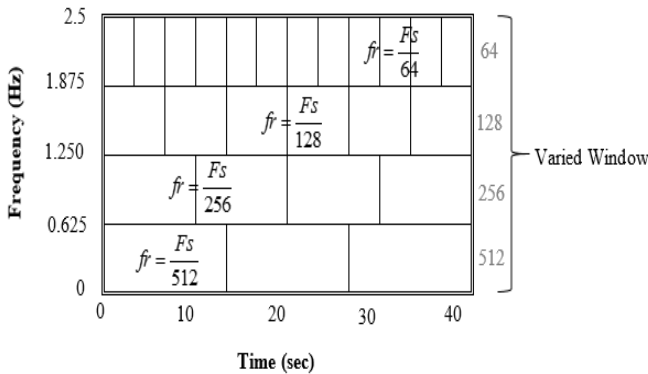


Fig. 2 ST resolution

C. Battery Parameters

Parameters of the battery were estimated from the TFR obtained using ST technique. The parameters at DC and AC components were measured instantaneously over time for battery lifetime prediction.

D. Instantaneous Means Square Voltage

The instantaneous means square voltage is a parameter that calculates the signal from frequency of 0 Hz to maximum frequency measured by using ST. $V_{RMS}(t)$ includes the overall parameters that occur at DC and AC components. The $V_{RMS}(t)$ can be expressed as

$$V_{RMS}(t) = \sqrt{\int_0^{f_{max}} ST_x(t, f) df} \quad (8)$$

where $ST_x(t, f)$ is the signal from TFR and f_{max} is the maximum frequency measured.

E. Instantaneous Direct Current Voltage

DC parameter can be estimated based on the area obtained from the fundamental frequency bandwidth of the battery. The fundamental frequency of the battery occurs at the highest magnitude of the ST. The instantaneous direct current voltage ($V_{DC}(t)$) [42] is expressed as

$$V_{DC}(t) = \sqrt{\int_{f_1 - \frac{\Delta f}{2}}^{f_1 + \frac{\Delta f}{2}} ST_x(t, f) df} \quad (9)$$

where f_1 is fundamental frequency that corresponds to system frequency and Δf is fundamental frequency bandwidth.

F. Instantaneous Alternating Current Voltage

The instantaneous alternating current voltage ($V_{AC}(t)$) is the voltage that appears at the frequency components. The $V_{AC}(t)$ can be calculated using

$$V_{AC}(t) = \sqrt{V_{RMS}(t)^2 - V_{DC}(t)^2} \quad (10)$$

III. RESULTS AND DISCUSSION

This section presents the results of battery charging/discharging signal analysis using ST. In this study, the charging/discharging signals for LA battery were run for 5 cycles, measured in between 0 second to 9000 seconds, as indicated in Fig. 3. A fixed conversion of charging and discharging cycle was set for every 1800 seconds until 5 battery cycles was achieved. The choice of charging and discharging time and current needed to be based on the capabilities of battery to forbear the overcharge and over discharge that cause inaccurate in measurements. In this study, charging/discharging current was set to fixed value of 1 A. The charging and discharging characteristics of the battery would be based on Equations (1), (2) and (3) simulated in MATLAB Simulink. Through ECM model, the battery was assumed to operate with constant nominal capacity, constant internal resistance, no memory effect, no temperature effect and unlimited cycle life.

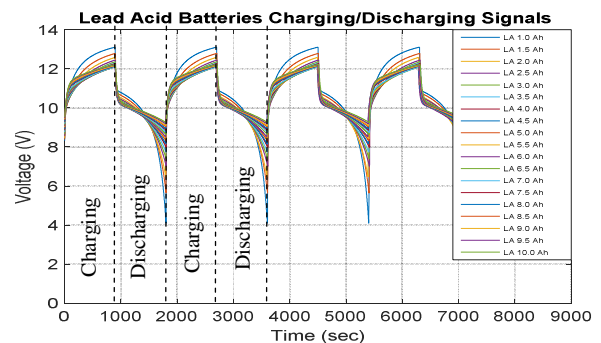


Fig. 3 Simulation of voltage charging/discharging signal for 12V LA batteries

The charging/discharging signals for LA battery with capacity of 1.0 Ah to 10.0 Ah are shown in Fig. 3. During the charging process, the 1.0 Ah battery voltage rose the highest compared to other batteries. The 1.0 Ah battery voltage gave the value of 13.11 V at maximum after 900 seconds of charging process, followed by 12.59 V for a 2.0 Ah battery and 12.36 V for a 3.0 Ah battery. The voltage for LA batteries kept decreasing, though from maximum, as the capacity was increased. When the batteries were being discharged, the 7.0 Ah battery voltage drained for about 3.354 V from 12.09 V. The signal pattern showed that the voltage for low battery capacity rose faster during the charging process, and drained rapidly when discharging process was conducted.

A. Battery Analysis for Parameters Estimation

This section discussed the battery charging/discharging signals analysis using TFD namely ST. From the ST technique, the best window length is chosen in extracting the signal information. The window length may affect the signal characteristics from the TFR where narrow window length may provide good time resolution while wide window length provide good frequency resolution. Selecting wider window length is recommended in battery signal analysis as the signal information requires high frequency resolution in determining the battery characteristics at AC components. The use of multi resolution analysis in ST technique gives benefit in battery signal analysis. The information at AC and DC components can be obtained in high accuracy value.

Different capacity of battery gives different charging and discharging magnitude. Fig. 4a shows the 1.0 Ah charging/discharging signals of the battery while Fig. 4b shows the results of the ST, presented in the three-dimensional plot in of signal energy with respect to time and frequency. The y-axis indicates the frequency of the battery while the x-axis represents the time measured in hour. The amplitude of the signal can be determined by the colour of the graph. The dark blue line represents the lowest amplitude and dark yellow indicates highest signal amplitude. This observation window signifies that the TFR graph appears constant over time duration from 0 to 9000 seconds.

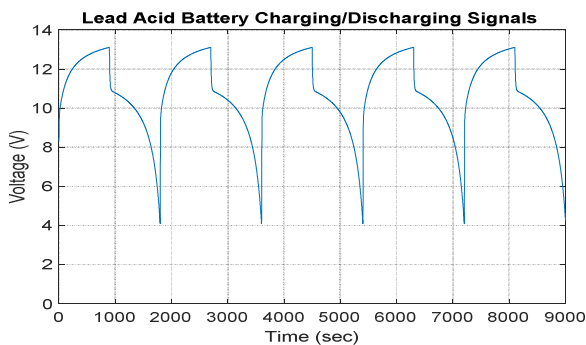


Fig. 4a 1.0 Ah LA charging/discharging signals

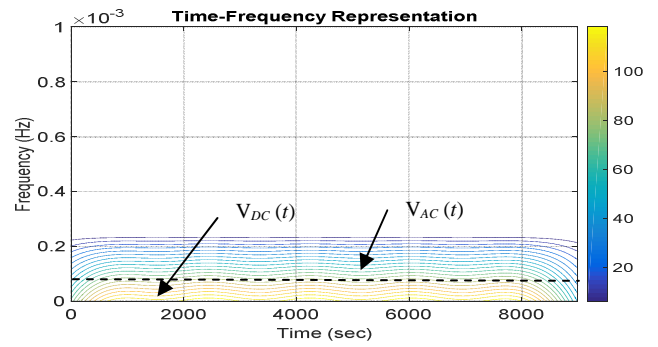


Fig. 4b TFR using ST for 1.0 Ah LA battery

From the TFR, battery parameters were estimated from the separation of DC and AC components. The value of $V_{DC}(t)$ was 10.9710 V while the value of $V_{AC}(t)$ was 0.9691 V as illustrated in Fig. 4c. The small value of $V_{AC}(t)$ was measured from the charging/discharging characteristics of the battery as shown in Fig. 4a. Since the battery was a DC source, which was 0 Hz at fundamental, the $V_{DC}(t)$ appeared higher.

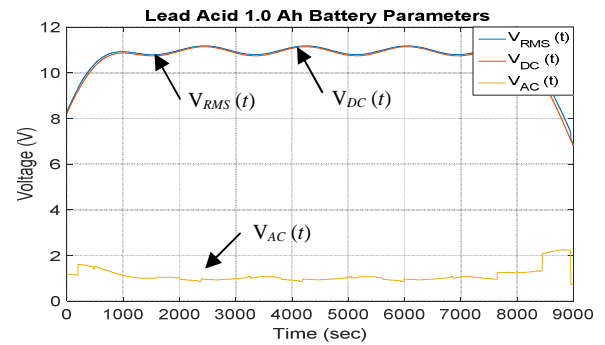


Fig. 4c Parameters for 1.0 Ah battery

Fig. 5a shows that the maximum voltages measured from charging/discharging signals for a 5.0 Ah battery was 12.18 V, which was 0.93 V less than by a 1.0 Ah battery (see Fig. 4a). The charging/discharging signal showed that with higher battery capacity, the maximum voltage of the battery would be lower. Fig. 5b indicates the TFR obtained using ST. The DC component of the battery was at 0 Hz, represented in yellow color, while the AC components were at higher frequency order.

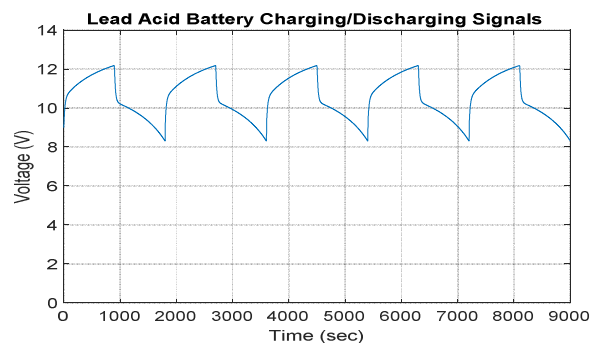


Fig. 5a 5.0 Ah LA charging/discharging signals

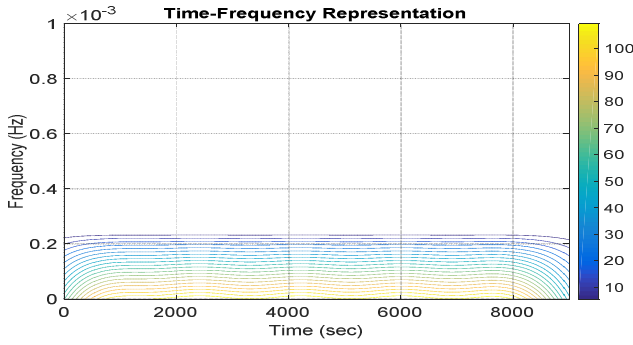


Fig. 5b TFR using ST for 5.0 Ah LA battery

From Fig. 5c, the $V_{RMS}(t)$ estimated is 10.6226 V, which consists of the values of $V_{DC}(t)$ and $V_{AC}(t)$. The $V_{AC}(t)$ estimated from the TFR seemed to give lower value compared to 1.0 Ah battery which was at 0.4165 V. The simulation process was repeated until 10.0 Ah parameters could be estimated with the increment of 0.1 Ah.

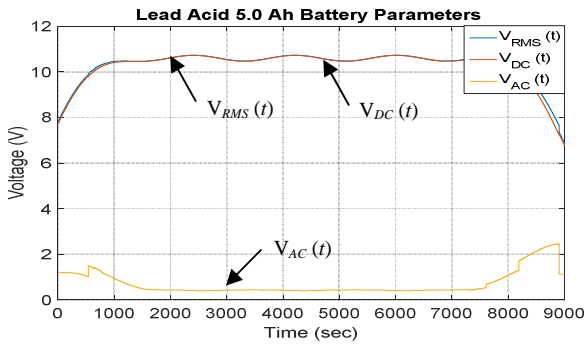


Fig. 5c Parameters for 5.0 Ah battery

In this section, batteries with 1.0 Ah and 5.0 Ah capacity are used as example in presenting the analysis signals in TFR for magnitude and frequency. Fig. 4a shows the charging/discharging signals of 1.0 Ah LA battery while Fig. 4b indicates its TFR obtained using ST technique. Using multi-resolution Gaussian kernel gives benefit to TFR in estimating the battery parameters of $V_{DC}(t)$ and $V_{AC}(t)$ accurately. As can be seen from Fig. 4c, the parameters for $V_{RMS}(t)$, $V_{DC}(t)$ and $V_{AC}(t)$ are estimated after the TFR is normalized which is between 1000 to 8000 seconds. This phenomena happen because of the use of Gaussian kernel in capturing the signals. Results from the ST technique shows the TFR appears to be good in both frequency and time resolution where the characteristics of charging/discharging still can be seen (see Fig. 3) that appears constant over time during normalized.

B. Performance Evaluation of Battery Characteristic

Signal characteristic is estimated from the calculation of signal parameter using ST techniques. For the calculation of alternating current voltage, the signal characteristics such as remaining capacity can be estimated. In this paper, the signal characteristics are obtained from the measurement of the battery charging/discharging from fixed rated voltage with varied capacities. The capacity of the battery depends

on the $V_{AC}(t)$ value which can be numerically identified that gives an advantage to estimate the SOC of the battery.

From Fig. 6, as the $V_{AC}(t)$ increase, the capacity growth exponentially. From 1 Ah to 2 Ah batteries, the gap of $V_{AC}(t)$ with the increment of 0.1 is wide and keep narrow until 10 Ah is achieved. This value is affected by the charging and discharging magnitude based on Fig. 3. For LA battery, the battery characteristics curve for $V_{AC}(t)$ ranges between 0.3 V to 1 V. The $V_{AC}(t)$ is dropping as the capacity is increased.

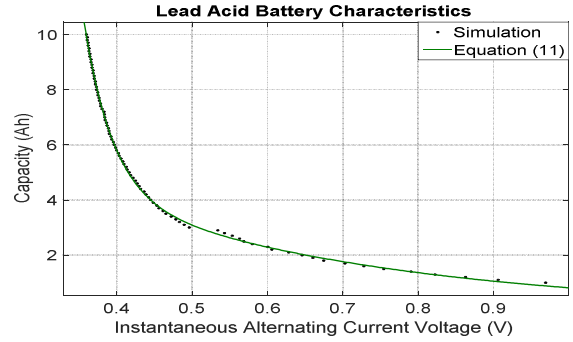


Fig. 6 Battery storage capacity of 1.0 Ah 10.0 Ah of simulation result for LA battery

From the simulation curve as shown in Fig. 6, Equation 11 was produced based on curve fitting tool simulated using MATLAB. The expected $V_{AC}(t)$ -capacity relationship naturally changed as the charging and discharging current were changed. The current production of the battery could be maximized if the $V_{AC}(t)$ of the battery was lower. The battery capacity was calculated using

$$Q_{LAS-transform}(V_{AC}) = 7.234 \times 10^4 \exp^{-26.26V_{AC}} + 10.62 \exp^{-2.566V_{AC}} \quad (11)$$

where Q is battery remaining capacity and V_{AC} is alternating current voltage.

IV. CONCLUSION

The evolution in portable appliances has focused to ensure battery capability to deliver high energy in a long period of time. This issue arises due to repeated use of secondary batteries, which leads to performance degradation, and consequently affects investment cost, environmental friendly and overall system performance. In this paper, testing based on IEEE standard have been conducted to analyze the battery charging/discharging signals and characteristics. The charging/discharging signals of the LA battery generated from the ECM can be used to estimate battery parameters. By applying ST signal processing technique, the analysis on charging/discharging signal will lead to parameters estimation at DC and AC components, i.e. $V_{RMS}(t)$, $V_{DC}(t)$ and $V_{AC}(t)$ through the TFR. This technique is capable to estimate the battery capacity from the $V_{AC}(t)$, to obtain the characteristics of LA battery with capacity of 1.0 Ah to 10.0 Ah. This technique is reliable for real-time monitoring system, as the equations and curve fitting tools involved are capable to estimate the remaining capacity of a battery.

NOMENCLATURE

| | |
|--------------|---|
| <i>LA</i> | Lead acid |
| <i>IEEE</i> | Institute of Electrical and Electronics Engineers |
| <i>SOC</i> | State of charge |
| <i>SOD</i> | State of discharge |
| <i>ST</i> | S-transform |
| <i>STFT</i> | Short time Fourier transform |
| <i>TFD</i> | Time-frequency distribution |
| <i>TFR</i> | Time-frequency representation |
| $V_{AC}(t)$ | Instantaneous of alternating current voltage |
| $V_{DC}(t)$ | Instantaneous of direct current voltage |
| $V_{RMS}(t)$ | Instantaneous of means square voltage |
| <i>WT</i> | Wavelet transform |

ACKNOWLEDGMENT

The authors would like to thank Universiti Teknikal Malaysia Melaka (UTeM), UTeM Zamalah Scheme and the Ministry of Higher Education (MOHE) for providing the research grant RAGS/1/2015/TK0/FKE/03/B00091 for this research. Special thanks to Advanced Digital Signal Processing Laboratory (ADSP), CeRIA for giving the support in this study.

REFERENCES

- [1] Pavlov, D. (2011). *Lead-acid batteries: science and technology*. Elsevier.
- [2] Praisuwanna, N., & Khomfoi, S. (2013, September). A seal lead-acid battery charger for prolonging battery lifetime using superimposed pulse frequency technique. In *Energy Conversion Congress and Exposition (ECCE), 2013 IEEE* (pp. 1603-1609). IEEE.
- [3] Praisuwanna, N., & Khomfoi, S. (2013, September). A seal lead-acid battery charger for prolonging battery lifetime using superimposed pulse frequency technique. In *Energy Conversion Congress and Exposition (ECCE), 2013 IEEE* (pp. 1603-1609). IEEE.
- [4] Xiang, C., Wu, S., Wang, W., & Zhao, F. (2013, October). A research on charge and discharge strategy of hybrid batteries based on the electrochemical characteristics. In *Telecommunications Energy Conference/Smart Power and Efficiency(INTELEC), Proceedings of 2013 35th International* (pp. 1-5). VDE.
- [5] Li, P., Pan, Y., Ma, Y., & Qin, Q. (2011, August). Study on an active voltage equalization charge system of a series battery pack. In *Electronic and Mechanical Engineering and Information Technology (EMEIT), 2011 International Conference on* (Vol. 1, pp. 141-144). IEEE.
- [6] Pachori, R. B., & Sircar, P. (2007). A new technique to reduce cross terms in the Wigner distribution. *Digital Signal Processing*, 17(2), 466-474.
- [7] Lee, L. C., Liong, C. Y., & Jemain, A. A. (2016). Applying Fourier-Transform Infrared Spectroscopy and Self-Organizing Maps for Forensic Classification of White-Copy Papers. *International Journal on Advanced Science, Engineering and Information Technology*, 6(6), 1033-1039..
- [8] Kasim, R., Abdullah, A. R., Selamat, N. A., Baharom, M. F., & Ahmad, N. H. T. H. (2015). Battery Parameters Identification Analysis Using Periodogram. In *Applied Mechanics and Materials* (Vol. 785, pp. 687-691). Trans Tech Publications.
- [9] He, H., Xiong, R., Zhang, X., Sun, F., & Fan, J. (2011). State-of-charge estimation of the lithium-ion battery using an adaptive extended Kalman filter based on an improved Thevenin model. *IEEE Transactions on Vehicular Technology*, 60(4), 1461-1469.
- [10] Mittal, D., O.P. Mahela and R. Jain, 2012. "Classification of Power Quality Disturbances in Electric Power System: A Review," IOSR Journal of Electrical and Electronics Engineering, 3: 06-14.
- [11] Axelberg, G.I.Y., P.G.V. and M.H.J. Bollen, 2007. "Support Vector Machine for classification of voltage disturbances," in IEEE Trans. Power Delivery, 2007, pp: 1297-1303.
- [12] Huda, N. H. T., Abdullah, A. R., & Jopri, M. H. (2013, June). Power quality signals detection using S-transform. In *Power Engineering and Optimization Conference (PEOCO), 2013 IEEE 7th International* (pp. 552-557). IEEE.
- [13] Nasrul, N., & Firmansyah, F. (2015). Harmonics Impact a Rising Due to Loading and Solution ETAP using the Distribution Substation Transformer 160 kVA at Education and Training Unit in PT PLN. *International Journal on Advanced Science, Engineering and Information Technology*, 5(6), 469-474.
- [14] Chassaing, R. 2005, *Digital Signal Processing and Applications with the C6713 and C6416 DSK*, John Wiley & Sons, Incorporated.
- [15] Gubanski, S. & Hartings, R. 1995. Swedish Research on the Application of Composite Insulators In Outdoor Insulation. *Electrical Insulation Magazine*, IEEE, 11, 24-31.
- [16] Gabor, D. (1946). Theory of communications. *IEEE Transactions on Signal Processing*, 12(1), 429-457.
- [17] Gargoom, A.M., Ertugrul, N. and Soong, W.L. 2007, Investigation of Effective Automatic Recognition Systems of Power-Quality Events. *Power Delivery*, IEEE Transactions on, vol. 22, no. 4, pp. 2319-2326.
- [18] Qian, S. & Chen, D. 1993. Discrete Gabor transform. *Signal Processing*, IEEE Transactions on, 41, 2429-2438.
- [19] Kasim, R., Abdullah, A. R., Selamat, N. A., & Bahari, N. (2015). Lithium-ion Battery Parameter Analysis Using Spectrogram. *Australian Journal of Basic and Applied Sciences*, 9(12), 76-80.
- [20] Chen, G., Chen, J., Dong, G., and Jiang, H., 2015. An adaptive non-parametric short-time Fourier transform: Application to echolocation. *Applied Acoustics*, 87, pp.131-141.
- [21] Saad, N. M., Rahman, N. N. S. A., Abdullah, A. R., Syafeeza, A. R., & Noor, N. S. M. (2017). Quadratic Distance and Level Classifier for Product Quality Inspection System. In *Proceedings of the International MultiConference of Engineers and Computer Scientists* (Vol. 1)..
- [22] Courmontagne, P., Ouelha, S., & Chaillan, F. (2012). On time-frequency representations for underwater acoustic signal. In *2012 Oceans*.
- [23] Moussa, A. E., Ei-Gammal, M., Abdallah, E. N. & Ei-Seoud, A. A. Hardware - software structure for on-line power quality assessment: part I. Rail Conference, 2004. Proceedings of the 2004 ASME/IEEE Joint, 8-8 April 2004 2004. 147-152.
- [24] An Approach For De-noising The Color Image Using Hybrid Wavelets, *International Journal of Application or Innovation in Engineering & Management (IJAIEM)*, Volume 3, Issue 5, May 2014.
- [25] Liu, Chun-Liu A Tutorial of The Wavelet Transform, 23 February 2010.
- [26] Abdullah, A. R., Sha'ameri, A. Z., Said, M., Ain, N., Mohd Saad, N., & Jidin, A. (2012). Bilinear time-frequency analysis techniques for power quality signals.
- [27] C M Leavey, M N James, J. Summerscales and R Sutton, An introduction to wavelet transforms: a tutorial approach, *Insight Vol 45* No 5 May 2003.
- [28] Karen Lees, "Image Compression Using Wavelets", May 2002.
- [29] S. Santoso, J. P. Edward, W. M. Grady, and A. C. Parsons, "Power Quality Disturbance Waveform Recognition Using Wavelet-Based Neural Classifier—Part 1: Theoretical foundation," *IEEE Trans. Power Delivery*, Vol.15, pp. 222-228, Feb. 2000.
- [30] J. V. Wijayakulasooriya, G. A. Putrus, and P. D. Minns, "Electric Power Quality Disturbance Classification Using Self-Adapting Artificial Neural Networks". *Generation, Transmission and Distribution, IEE Proceedings*, Vol. 149, No. 1, pp. 98-101, Jan. 2002
- [31] Abdullah, A. R., & Sha'ameri, A. Z. (2010, May). Power quality analysis using smooth-windowed wigner-ville distribution. In *Information Sciences Signal Processing and their Applications (ISSPA), 2010 10th International Conference on* (pp. 798-801). IEEE.
- [32] Stockwell, R. G., Mansinha, L., & Lowe, R. P. (1996). Localization of the complex spectrum: the S transform. *IEEE transactions on signal processing*, 44(4), 998-1001.
- [33] Tadi, M. J., Lehtonen, E., Lahdenoja, O., Pankaala, M., & Koivisto, T. (2016, October). An adaptive approach for heartbeat detection based on S-transform in seismocardiograms. In *Engineering in Medicine and Biology Society (EMBC), 2016 IEEE 38th Annual International Conference of the* (pp. 2370-2373). IEEE.

- [34] Mukhopadhyay, S., Ghosh, N., Barman, R., Panigrahi, P. K., Pratiher, S., & Pradhan, A. (2016, January). S-transform based fluctuation analysis-a method for pre-cancer detection. In *Microelectronics, Computing and Communications (MicroCom)*, 2016 International Conference on (pp. 1-5). IEEE.
- [35] Huang, Z. L., Zhang, J., Zhao, T. H., & Sun, Y. (2016). Synchrosqueezing S-transform and its application in seismic spectral decomposition. *IEEE Transactions on Geoscience and Remote Sensing*, 54(2), 817-825.
- [36] Zhu, H., Brown, R. A., Villanueva, R. J., Villanueva, J., Lauzon, M. L., Mitchell, J. R., & Law, A. G. (2004). Progressive imaging: S-transform order. *ANZIAM Journal*, 45, 1002-1016.
- [37] Suja, S., & Jerome, J. (2010). Pattern recognition of power signal disturbances using S Transform and TT Transform. *International journal of electrical power & energy systems*, 32(1), 37-53.
- [38] Cohen, L. 1989. *Time-Frequency Distributions-A Review*. *Proceedings of The IEEE*, 77, 941-981.
- [39] Melentjev, S. and D. Lebedev, Overview of Simplified Mathematical Models of Batteries. *Egdk. Ttu. Ee*, pp: 231-235.
- [40] Ibrahim, A. E., Kawady, T. A., Darwish, H. A. & Taalab, A. M. Generalized 1-D Gabor Transform Application To Power System Signal Analysis. *Industrial Electronics, 2006 IEEE International Symposium On*, 9-13 July 2006 2006. 624-629.
- [41] Bigliassi, M., Scalassara, P. R., Kanthack, T. F. D., Abrão, T., de Moraes, A. C., & Altimari, L. R. (2014). Fourier and Wavelet Spectral Analysis of EMG Signals in 1-km Cycling Time-Trial. *Applied Mathematics*, 2014.
- [42] Zawawi, T. N. S. T., Abdullah, A. R., Shair, E. F., Halim, I., & Rawaida, O. (2013, December). Electromyography signal analysis using spectrogram. In *Research and Development (SCORED)*, 2013 IEEE Student Conference on (pp. 319-324). IEEE.